

## Energy flow of moving dissipative topological solitons

A. V. Gorbach, S. Denisov, and S. Flach

Max-Planck-Institut für Physik komplexer Systeme, Nöthnitzer Strasse 38, 01187 Dresden, Germany

(Received 11 January 2006; accepted 2 May 2006; published online 23 June 2006)

We study the energy flow due to the motion of topological solitons in nonlinear extended systems in the presence of damping and driving. The total field momentum contribution to the energy flux, which reduces the soliton motion to that of a point particle, is insufficient. We identify an additional *exchange* energy flux channel mediated by the spatial and temporal inhomogeneity of the system state. In the well-known case of a dc external force the corresponding exchange current is shown to be small but nonzero. For the case of ac driving forces, which lead to a soliton ratchet, the exchange energy flux mediates the complete energy flow of the system. We also consider the case of combination of ac and dc external forces, as well as spatial discretization effects. © 2006 American Institute of Physics. [DOI: 10.1063/1.2207307]

**Solitons represent one of the striking and famous aspects of nonlinear phenomena in spatially extended systems studied during more than half a century. Moving solitons transport energy in a coherent and particle-like way for integrable systems. Departure from integrability, especially when including dissipation, introduces novel features of soliton dynamics which are different from that of a point particle. In this article we study the influence of the nonlocality of a dissipative topological soliton on the balance of energy flows. Especially we show that the total energy flow is realized along two pathways—the total internal momentum and an exchange current between the soliton field and the external degrees of freedom which are responsible for the dissipation. For the case of an external ac force the moving soliton (ratchet effect) transports energy exclusively via the exchange current, whereas the total field momentum vanishes exactly. Even for the long-studied case of a constant external force the exchange current does not vanish. These findings unambiguously demonstrate that a moving dissipative soliton represents a collective field excitation whose dynamics cannot be reduced to that of a point particle.**

### I. INTRODUCTION

Solitary waves or solitons represent one of the striking and famous aspects of nonlinear phenomena in spatially extended systems. They appear as specific types of localized solutions of various nonlinear partial differential equations and possess several important properties.<sup>1</sup> These properties include an exponential localization of energy remaining unchanged during soliton propagation, and an elastic scattering of solitons. The latter one, i.e., the fact that two solitary waves maintain their identity after collisions, inspired the introduction of the term *soliton*,<sup>2</sup> which emphasizes the analogy between these objects and particles. Later it has been realized, however, that an essential condition for the particle-like behavior of solitons is the integrability of the corresponding models. But the effect of dynamical localization of energy was found to be much more general, and the notion of soliton has been extended nowadays to nonintegrable models

as well. An analogy between such “generalized” solitons and particles is less obvious. Not only the scattering process is generally different from the elastic scattering of particles, but several other important physical effects may appear for solitary waves in nonintegrable models. An important feature essentially breaking the particle approach to soliton dynamics is connected with the possibility of excitation of the so-called *shape*<sup>3</sup> or *internal*<sup>4</sup> modes: in contrast to a rigid body, a soliton may perform shape oscillations while propagating. The mechanism of possible energy exchange between the soliton kinetic energy, associated with its translational motion, and the internal energy of shape modes, can drastically change the soliton dynamics and leads in some cases to resonances during soliton-soliton interactions.<sup>3</sup>

Another important aspect of soliton dynamics in nonintegrable systems, which we address in this article, concerns the problem of energy transport associated with a directed soliton propagation. As a soliton carries some (finite) nonzero energy, it is naturally to assume that its translational motion would result in a nonzero energy current in the system. One can introduce a *total field momentum*, in analogy to a particle mechanical momentum, which precisely corresponds to the energy current when considering solitons in integrable systems.<sup>1</sup> However, an attempt to extend this momentum-based approach to dissipative solitons may lead to confusing and misleading results. As an example, we mention here the so-called soliton ratchets: the effect of a unidirectional motion of a topological soliton (kink) under the influence of a spatially homogeneous and time-periodic external bias with zero mean.<sup>5–13</sup> As an extension of single particle ratchets,<sup>14</sup> at a first glance soliton ratchets demonstrate at least qualitatively a nice analogy between solitons and particles. Indeed, applying the same symmetry analysis as for particle ratchets,<sup>15</sup> one observes a directed motion of kinks not only in numerical simulations, but also in experiments with annular Josephson junctions.<sup>12,13</sup> However, a surprising and puzzling result appears if one estimates the energy current for the soliton ratchet case: simple analytical calculations tell that the averaged value of the total field

momentum is strictly equal to zero.<sup>16,17</sup> An analogous effect of nontopological soliton motion with zero total field momentum has been reported also for a nonlinear Schrödinger equation with parametric driving in the presence of dissipation.<sup>18</sup> These results show, that the total field momentum is no longer an adequate quantity to describe the energy flow due to soliton dynamics in nonintegrable damped and driven systems.

In this article we study the energy flow due to soliton dynamics in the framework of the sin-Gordon model with a spatially homogeneous external driving and damping. We show, that in general the energy current associated with a translational motion of the topological soliton (kink) consists of two contributions. The above-mentioned total field momentum constitutes only one component of the total current—the *internal* current. Another path for energy transport in the system is mediated by an inhomogeneous in time and space energy exchange between the soliton and the external degrees of freedom (driving force and damping). The corresponding *exchange* current has no analogy within the particle description of a moving soliton. Its existence is solely due to the spatial extent of the soliton. Even for the case of a time-independent driving, when shape modes are not excited, the exchange current is small but nonzero. It is drastically enhanced by the excitation of shape modes via a time-periodic driving or a spatial discretization of the system.

The article is organized as follows: In Sec. II we introduce the driven and damped sin-Gordon model and the basic definitions of the energy balance equation and the total field momentum (internal energy current). In Sec. III the case of soliton motion under the influence of a dc external force is discussed. We demonstrate, that the internal energy current does not account for the total energy flow in the system. We introduce the notion of the exchange current, which completes the energy flow balance. A generalization of our approach to the case of soliton motion induced by ac driving forces (soliton ratchet) is given in Sec. IV. The effects of discretization are discussed in Sec. V. Finally, Sec. VI concludes the article.

## II. THE MODEL

We consider a topological soliton (kink) motion in the driven and damped sin-Gordon model,<sup>19</sup> widely used in the field of soliton ratchets,<sup>5,8–12</sup> which describes the dynamics of the superconducting phase difference across the annular Josephson junction<sup>12</sup>

$$\varphi_{tt} - \varphi_{xx} = -\alpha\varphi_t - \sin\varphi + E(t). \quad (1)$$

This equation describes the evolution of a scalar field  $\varphi$  in space and time. Here and in what follows, subscripts  $x$  and  $t$  denote partial derivatives with respect to the corresponding variables. The parameter  $\alpha$  regulates the strength of damping in the system, and  $E(t)$  is an external driving force. In addition, we impose the kink-bearing periodic boundary condition

$$\varphi(x+L, t) = \varphi(x, t) + Q, \quad \varphi_t(x+L, t) = \varphi_t(x, t), \quad (2)$$

where  $Q=2\pi$  is the topological charge and  $L$  is the system size.

The field energy density is given by

$$\rho[\varphi(x, t)] \equiv \rho(x, t) = \frac{1}{2}(\varphi_t^2 + \varphi_x^2) + 1 - \cos(\varphi). \quad (3)$$

Its dynamics is governed by the following energy balance equation:

$$\rho_t = -j_x^I - \alpha\varphi_t^2 + E(t)\varphi_t. \quad (4)$$

Here we introduce the *internal energy current*  $J^I(t)$  and its density  $j^I(x, t)$ :

$$J^I(t) = \int_0^L j^I dx, \quad j^I(x, t) = -\varphi_x\varphi_t. \quad (5)$$

$J^I$  is also known in the literature as the total field momentum.<sup>19–22</sup> By differentiating Eq. (5) and using Eq. (1) together with the boundary condition (2) it is straightforward to show<sup>17,20,21</sup> that the internal current  $J^I$  satisfies the following ordinary differential equation:

$$J_t^I(t) = -\alpha J^I(t) - QE(t). \quad (6)$$

In the absence of an external force  $E(t) \equiv 0$  and dissipation  $\alpha \equiv 0$  (i.e., in the *nonperturbed* integrable sin-Gordon model), Eq. (1) with the previous boundary conditions (2) supports the well-known kink solution,<sup>19</sup> which in the limit of an infinite system size  $L \rightarrow \infty$  takes the form

$$\varphi^{\text{kink}}(x, t) = 4 \arctan \left\{ \exp \left[ \frac{x - Vt}{\sqrt{1 - V^2}} \right] \right\}, \quad (7)$$

where  $V$  is the kink velocity,  $|V| < 1$ . According to the energy balance equation (4), in this case the internal energy current  $J^I$  is the only possible pathway to mediate an energy transport in the system. Using the expression (7) for the kink solution and the definitions of the internal energy current  $J^I$  (5) and energy density  $\rho$  (3), it follows, that the energy current associated with the kink motion can be obtained in full analogy with a moving point particle

$$J^I \equiv VW^{\text{kink}}. \quad (8)$$

Here the kink energy  $W^{\text{kink}}$  is obtained from the energy density  $\rho(\varphi)$ ,

$$W^{\text{kink}} = \int_0^L \rho[\varphi^{\text{kink}}] dx, \quad W_{L \rightarrow \infty}^{\text{kink}} = \frac{8}{\sqrt{1 - V^2}}. \quad (9)$$

In the general case, when both  $E$  and  $\alpha$  are nonzero, a moving kink solution of Eq. (1) can persist as an attractor of the system with all the parameters (including the kink velocity) determined by the choice of  $E$ ,  $\alpha$ , and  $L$ . Our goal is to compute the energy current generated by such a moving kink. As will be shown below, an inhomogeneous exchange of energy between the kink and the external degrees of freedom (force and dissipation), opens an additional path for energy transport in the system, which, together with the previous internal current, constitute the full energy current balance generated by the moving kink.

### III. CONSTANT DRIVING FORCE

Let us start with the seemingly simple case of the perturbed sin-Gordon equation (1)—the case of a constant driving force  $E(t)=E\equiv\text{const.}$ . A kink moves in this case with a constant velocity  $V$  (defined by a choice of the force strength  $E$ , as well as the damping constant  $\alpha$  and the system length  $L$ ), so that the corresponding attractor solution depends only on a single variable  $\xi=x-Vt$ ,<sup>19</sup>

$$\varphi(x,t) = \psi(x - Vt) \equiv \psi(\xi). \tag{10}$$

Due to the time homogeneity the total energy of the system  $W$ ,

$$W = \int_0^L \rho[\varphi(x,t)] dx, \tag{11}$$

remains constant in time on the attractor solution. For a point particle the current balance would not change, as the energy loss due to the damping would be compensated by the external dc field. For the spatially extended kink this will not be the case anymore.

Let us assume, that the system size  $L$  is chosen to be large enough, so that far away from the kink center the spatial field distribution asymptotically approaches the homogeneous ground state:  $\psi(\xi \rightarrow 0) \rightarrow \phi^v$ ,  $\psi(\xi \rightarrow L) \rightarrow \phi^v + Q$ . Note, that the external force  $E$  shifts the degenerate ground state of the system from  $\varphi_G^{(0)} = 2\pi m, m=0, \pm 1, \pm 2, \dots$  to  $\varphi_G^{(E)} = \varphi_G^{(0)} + \varphi^v(E)$ ,  $\varphi^v(E) \equiv \arcsin(E)$ .

We denote by  $w(x,t)$  the amount of energy stored on the stripe  $[0,x]$  at time  $t$ . We further assume that  $x=0$  is far from the kink center so that the energy current density vanishes there. Then we can define the local energy current density  $j(x,t)$  as

$$j(x,t) = - \frac{\partial w(x,t)}{\partial t} = - \int_0^x \rho_t(x',t) dx'. \tag{12}$$

Using the attractor property (10), we obtain

$$j(x - Vt) \equiv j(\xi) = V[\rho(\xi) - \rho(0)], \tag{13}$$

and the total energy current  $J$  is thus given by

$$J = \int_0^L j(\xi) d\xi \equiv V \left[ \int_0^L \rho(\xi) d\xi - L\rho(0) \right]. \tag{14}$$

The quantity in the square brackets on the right-hand side (rhs) of Eq. (14) is the difference between the system energy with and without the kink. Indeed, in the presence of external force and damping, the ground state energy has shifted from zero to  $W_0 = L\rho(\phi^v) = L\rho(x=0)$ . This difference is precisely the kink energy  $W^k = W - W_0$ . Thus, we arrive to the simple relation between the total energy current  $J$ , kink velocity  $V$ , and kink energy  $W^k$

$$J = VW^k. \tag{15}$$

As expected, this expression corresponds to that of a point particle moving with velocity  $V$  and carrying energy  $W^k$ . However, opposite to the integrable case  $E=\alpha=0$ , the internal current  $J^I$  does not coincide with the total current  $J$ :  $J^I \neq J$ . Indeed, using the definition of the total current  $J$  given

in Eqs. (12) and (14) and the energy balance equation (4), we arrive at

$$J = J^I + J^E, \tag{16}$$

where the *exchange current*  $J^{E16}$  has been introduced

$$J^E = V \int_0^L dx \int_0^x d\xi [\alpha V(\psi'(\xi))^2 + E\psi'(\xi)]. \tag{17}$$

Following the definition of the internal current  $J^I$  in Eq. (5), we obtain

$$J^I = V \int_0^L (\psi'(x))^2 dx, \tag{18}$$

so that all components of the current balance equation (16) are expressed through the field  $\psi$ . Below we will calculate numerically the moving kink attractor solution  $\psi(\xi)$  in order to estimate all the three currents for different values of the model parameters. Note, that according to Eq. (6) one can obtain the exact value for the internal current  $J^I$  on the attractor solution in an independent way,

$$J^I_{\text{exact}} = - \frac{EQ}{\alpha}. \tag{19}$$

We will use this expression in order to control the accuracy of our numerical schemes.

The fact that the moving kink solution  $\phi(x,t)$  depends only on the single variable  $\xi=x-Vt$  allows to reduce the original field equation (1) to the well studied driven and damped pendulum problem. Indeed, substituting ansatz (10) into Eq. (1), we arrive to the following ordinary differential equation (ODE) for the function  $\psi(\xi)$ ,

$$(1 - V^2)\psi'' = -\alpha V\psi' + \sin(\psi) - E, \tag{20}$$

which describes the evolution of an effective pendulum with the momentum of inertia  $M=(1-V^2)$ . The damping constant  $\gamma=\alpha V$  depends on the kink velocity  $V$ . The external force  $E$  plays the role of an applied constant torque to the pendulum. By introducing the effective time

$$\tau = \frac{\xi}{\sqrt{1 - V^2}}, \tag{21}$$

Eq. (20) can be finally rewritten for the function  $y(\tau) \equiv \psi(\xi/\sqrt{1-V^2})$ ,

$$\ddot{y} = -G\dot{y} + \sin(y) - E, \tag{22}$$

with the damping constant  $G$  defined through the original kink parameters:

$$G(E,L) = \frac{\alpha V(E,L)}{\sqrt{1 - V^2(E,L)}}. \tag{23}$$

Here we emphasize the implicit dependence of  $G$  on the strength of the external force  $E$  and the system size  $L$ , as the kink velocity  $V$  is unambiguously defined by these parameters.

Thus, a moving kink solution (10) of the original problem (1) with the boundary conditions (2) corresponds to a rotating solution  $\hat{y}(\tau)$  of the driven and damped pendulum

(22). On this solution the pendulum performs periodic rotations with the period  $T$  defined through the original system length  $L$  and the kink velocity  $V$  as

$$T = \frac{L}{\sqrt{1 - V^2}}. \tag{24}$$

Note also, that the limit of an infinite system size  $L$  corresponds to a separatrix solution of the pendulum with  $T \rightarrow \infty$ .

The existence and the characteristics of the rotating solution in Eq. (22) depend on the choice of values of  $G$  and  $E$ .<sup>24-26</sup> For each given value of  $E$  from the interval  $|E| \leq 1$  there is a critical value of  $G = G_{cr}(E)$ , below which the rotating solution coexists together with a stable static pendulum state (the latter corresponds to the homogeneous ground state in the kink tails). The period of the rotating solution tends to infinity as  $G$  approaches  $G_{cr}$  from below, whereas above the critical value of  $G$  the rotating solution disappears. As a consequence, the value  $G_{cr}(E)$  corresponds to the limit of an infinite size  $L$  in the original problem (1) with the corresponding drive  $E$ , whereas any lower value  $G < G_{cr}$  is associated with a moving kink in a finite-size system. For small values of  $|E|$  the critical value of the effective damping can be approximated as<sup>26</sup>

$$G_{cr} \approx \frac{\pi E}{4}, \quad |E| \ll 1. \tag{25}$$

By using relation (23) one can derive the corresponding approximation for the kink velocity in an infinite-size system at low power of the external drive,

$$V \approx \frac{\pi E}{\sqrt{16\alpha^2 + \pi^2 E^2}}, \quad |E| \ll 1. \tag{26}$$

To find the separatrix solution of (22) and the corresponding value of  $G_{cr}$  at arbitrary values of  $E$  we use the Newton-Raphson iterations of the shooting method in phase space  $(\dot{y}, y)$ , rewriting Eq. (22) as<sup>26</sup>

$$z(y) = \dot{y}, \tag{27}$$

$$\frac{dz}{dy} = -G + \frac{\sin(y) - E}{z}, \tag{28}$$

and computing the map

$$\{z(y_0), y_0\} \rightarrow \{z(y_0 + 2\pi), y_0 + 2\pi\}, \tag{29}$$

$$y_0 = \arcsin(E). \tag{30}$$

For any  $z_0 \equiv z(y_0)$  a unique solution of (27) and (28) satisfying condition  $z(y_0 + 2\pi) = z_0$  can be found by tuning the parameter  $G$ , provided that the sign of  $z_0$  is chosen in accordance with the sign of  $E$ . The critical value  $G_{cr}$  is obtained by taking  $z_0 = 0$ . Note, that the value of  $z_0$  is proportional to the value of  $\psi'(\xi = 0, L)$ . For any finite system size  $L$  it is non-zero due to exponentially decaying kink tails.

In Fig. 1 the computed values of  $G_{cr}$ , as well as the corresponding values of the kink velocity  $V$ , are shown with circles. In fact, the approximation for the kink velocity (26) works reasonably well even at values of  $E$  close to unity,

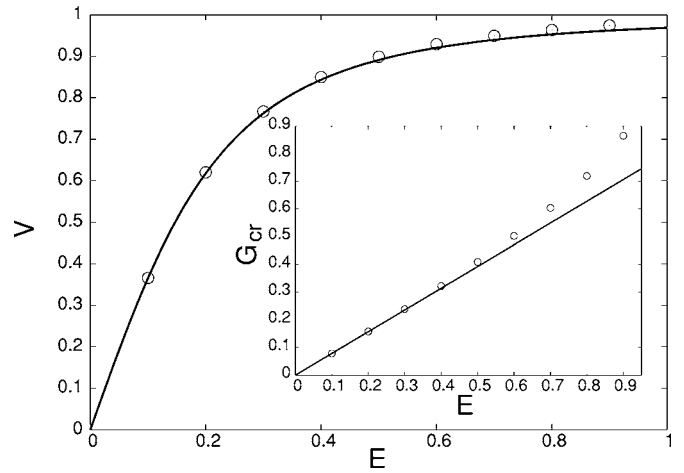


FIG. 1. Kink velocity as a function of the dc force  $E$  for  $\alpha=0.2$ . Numerical solution of (22), see the text for details (open circles) and approximative solution (26) (solid line). Inset: critical value  $G_{cr}$  from (23) for  $\alpha=0.2$ . Numerical solution (see text for details) (open circles) and approximative solution (25) (solid line).

whereas the critical value  $G_{cr}$  deviates stronger from the linear approximation (25) at values of the driving force close to  $E=1$ .

Once the separatrix solution  $\hat{y}(\tau)$  of (22) is found, the values of the total (14), exchange (17), and internal (18) currents for the corresponding moving kink solution can be obtained:

$$J^E = \frac{\alpha G}{\alpha^2 + G^2} (D - F), \tag{31}$$

$$J^I = \frac{2G}{\alpha} F, \tag{32}$$

$$J = \frac{G}{\alpha} \frac{\alpha^2 + 2G^2}{\alpha^2 + G^2} F + \frac{\alpha G}{\alpha^2 + G^2} D \equiv J^E + J^I, \tag{33}$$

where the functions  $F$  and  $D$ , are related to the mean pendulum kinetic and potential energies:

$$F(E, L) = \int_0^T d\tau \frac{\dot{y}^2}{2}, \tag{34}$$

$$D(E, L) = \int_0^T d\tau [\sqrt{1 - E^2} - \cos(y)]. \tag{35}$$

Here the implicit dependence on the original system length  $L$  comes through the pendulum period  $T$ .

Therefore, the three functions  $D$  (35),  $F$  (34) and  $G$  (23), uniquely defined for a rotating solution of (22) for a given value of the external field  $E$  and  $\dot{y}(0)$ , determine all the characteristics of the corresponding moving kink problem: its spatial profile, velocity, energy, internal, exchange and total currents. In Table I we list the values of all three currents calculated for the damping constant  $\alpha=0.2$  and different strength of the external driving force  $E$  by means of the pendulum approach, corresponding to the limit of  $L \rightarrow \infty$  in the original system (1). In order to control the accuracy of



TABLE I. The values of the internal, exchange and total currents for the damping constant  $\alpha=0.2$  and an infinite system size  $L \rightarrow \infty$ , calculated within the pendulum approach for  $G=G_{cr}$ .  $\Delta J^I$  and  $\Delta J$  are the errors of the calculated internal current and the accuracy at which the current balance relation (16) is fulfilled, respectively (see the main body text for details).

$E$	$J^I$	$J^E$	$J$	$ J^E/J $	$ \Delta J^I $	$ \Delta J $
-0.05	1.570 796 328	$-7.649\ 38 \times 10^{-4}$	1.570 031 391	$4.9 \times 10^{-4}$	$1.7 \times 10^{-9}$	$1.0 \times 10^{-10}$
-0.1	3.141 592 658	$-5.531\ 719 \times 10^{-3}$	3.313 606 094	$1.8 \times 10^{-3}$	$4.8 \times 10^{-9}$	$1.6 \times 10^{-10}$
-0.15	4.712 388 99	$-1.610\ 701 \times 10^{-2}$	4.696 281 98	$3.4 \times 10^{-3}$	$1.2 \times 10^{-8}$	$1.0 \times 10^{-9}$
-0.2	6.283 185 32	$-3.210\ 284 \times 10^{-2}$	6.251 082 48	$5.1 \times 10^{-3}$	$1.3 \times 10^{-8}$	$1.0 \times 10^{-9}$
-0.25	7.853 982 6	$-5.211\ 35 \times 10^{-2}$	7.801 869 1	$6.7 \times 10^{-3}$	$9.4 \times 10^{-7}$	$1.0 \times 10^{-8}$
-0.3	9.424 778 3	$-7.503\ 35 \times 10^{-2}$	9.349 744 8	$8.0 \times 10^{-3}$	$3.7 \times 10^{-7}$	$5.0 \times 10^{-8}$
-0.35	10.995 576	$-9.988\ 3 \times 10^{-2}$	10.895 692	$9.2 \times 10^{-3}$	$1.2 \times 10^{-6}$	$1.0 \times 10^{-7}$
-0.4	12.566 373	$-1.263\ 08 \times 10^{-1}$	12.440 065	$1.0 \times 10^{-2}$	$2.4 \times 10^{-6}$	$1.0 \times 10^{-7}$
-0.5	15.707 99	$-1.832\ 6 \times 10^{-1}$	15.524 72	$1.2 \times 10^{-2}$	$2.2 \times 10^{-5}$	$1.0 \times 10^{-6}$
-0.6	18.849 57	$-2.483\ 2 \times 10^{-1}$	18.601 26	$1.3 \times 10^{-2}$	$2.2 \times 10^{-5}$	$1.0 \times 10^{-6}$
-0.7	21.991 16	$-3.261\ 7 \times 10^{-1}$	21.665 00	$1.5 \times 10^{-2}$	$2.0 \times 10^{-5}$	$1.0 \times 10^{-6}$
-0.8	25.133 1	$-4.258 \times 10^{-1}$	24.707 3	$1.7 \times 10^{-2}$	$3.0 \times 10^{-4}$	$1.0 \times 10^{-5}$

our numerical scheme, we estimate the error of the calculated internal current  $|\Delta J^I|$ , for which we know the exact result  $J^I_{\text{exact}}$  (6). We also indicate in Table I the accuracy  $\Delta J$  which the current balance equation (16) is fulfilled,  $\Delta J = J - J^I - J^E$ , and the relative strength of the exchange current  $|J^E/J|$ .

To verify the pendulum approach, we performed direct numerical integration of the original system (1) with the initial condition in the form of stationary kink solution (7) of the unperturbed (integrable) sin-Gordon model.<sup>27</sup> Once variations of the total system energy (11) over any characteristic timescales become negligible (of the order of standard double precision numerical error), we assume that the system evolves in accordance to the moving kink attractor. Then all the currents are calculated following their original definitions (14), (5), and (17). We found perfect agreement with the results listed in Table I.

The surprising result of the presented analysis is that for the case of a constant driving force, when the kink is known to behave similar to a point particle without any internal degrees of freedom being excited, the exchange current is nonzero. It is relatively weak, but both its absolute value and its relative strength are significantly larger than the estimated numerical error and increase with increasing driving force  $E$ .

As for a constant driving force all currents are time independent, we can easily define the densities of internal and exchange currents

$$j^I(x) = V\psi'(x)^2, \quad (36)$$

$$j^E(x) = V \int_0^x d\xi [\alpha V(\psi'(\xi))^2 + E\psi'(\xi)], \quad (37)$$

using Eqs. (18) and (17). The corresponding profiles are plotted in Fig. 2 for the case  $\alpha=0.2$ ,  $E=0.2$ . First it is evident from (37), that the exchange current density is nonzero, similar to the internal current density (36). This is due to the finite spatial extent of the kink, which causes a corresponding spatially (and thus temporally as well) inhomogeneous energy exchange between the field  $\varphi$ , the external forcing  $E$  and the damping term. A total vanishing of  $J^E$  could only

hold due to some spatial symmetry of  $j^E(x)$  which in turn has to be generated by some symmetry of the kink profile. However the kink profile in the presence of driving force and damping is asymmetric. That is the main reason for the non-vanishing exchange current contribution.

Finally, we note, that the reduction to traveling solution (10) is valid only for the case of  $|E| \leq 1$ . Indeed, in the case of  $|E| > 1$  the rotating solution of (22) persist, but the stable fixed point disappears. This means that one no longer has a homogeneous ground state in the kink tails. Similarly, when  $|E| > 1$  the proposed scheme for the calculation of the total and exchange currents, Eqs. (14) and (17), breaks, as the homogeneous ground state in the kink tails is no longer supported by the starting equations.

#### IV. TIME-PERIODIC DRIVING FORCE: SOLITON RATCHETS

In this section we proceed to the case of a time-periodic driving force  $E(t+T)=E(t)$  with zero mean value. For the

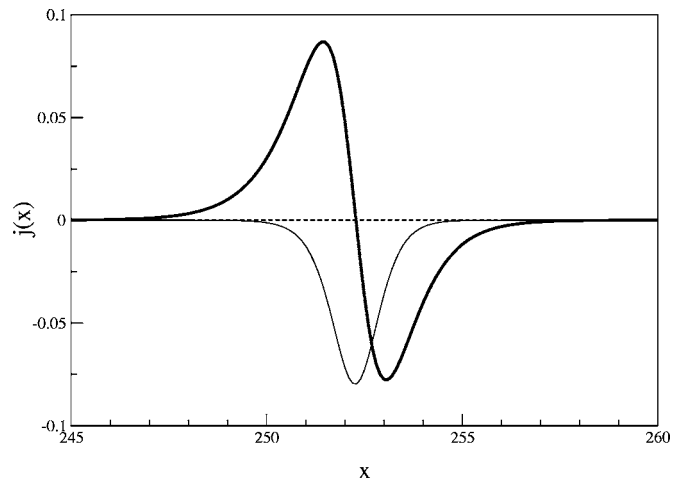


FIG. 2. The densities of the scaled internal current,  $0.02 j^I(x)$  (thin line), and of the exchange current,  $j^E(x)$  (bold line), for the  $E=0.2$ ,  $\alpha=0.2$  and  $L=500$ . The region near the kink center at  $x \approx 252$  is zoomed.

case of an ac driving force, which possesses the time-shift symmetry

$$E(t) = -E(t + T/2), \tag{38}$$

the combined symmetry transformation

$$x \rightarrow -x, \quad \varphi \rightarrow -\varphi + Q, \quad t \rightarrow t + \frac{T}{2} \tag{39}$$

leaves Eq. (1) invariant while changing the sign of the kink velocity  $V$  defined, e.g., as<sup>8,9</sup>

$$V(t) = \frac{1}{Q} \int_0^L x \varphi_{tx} dx. \tag{40}$$

If only one kink attractor persists, then on this attractor the kink will not move, but oscillate at the best.<sup>8,16</sup> This is the typical situation observed in various numerical simulations. In the unlikely case that a kink attractor persists on which the kink is moving with a nonzero average velocity, then by symmetry another attractor exists as well, on which the kink moves with the opposite velocity. However, the previous time-shift symmetry (38) is generally removed by choosing the biharmonic driving force

$$E(t) = E_1 \cos[\omega(t - t_0)] + E_2 \cos[2\omega(t - t_0) + \Theta], \tag{41}$$

$$\omega = \frac{2\pi}{T}, \quad 0 < \Theta < 2\pi.$$

As a consequence, the kink on the attractor solution will in general have a nonzero velocity (provided no other hidden symmetries of the system persist). This results in a unidirectional (in average) motion of the kink under the influence of zero-mean periodical driving force given in Eq. (41).<sup>8,9,16</sup> The corresponding kink ratchet effect was observed both in numerical simulations<sup>8,10</sup> and in experiments with an annular Josephson junction.<sup>12</sup> In Fig. 3(a) the characteristic evolution of the energy density (3) in the kink ratchet dynamics with the biharmonic driving force (41) is shown. A gradual drift of the energy density peak, associated with the kink center, is clearly observed.

The unidirectional motion of the kink should result in the appearance of a nonzero averaged energy current. Simultaneously, as follows from Eq. (6), for any zero-mean  $E(t)$ , the time average value of the internal current  $J^I$  should be zero on the attractor.<sup>17,20,21</sup> Therefore, the internal current does not contribute to the energy transport associated with the kink motion. This is impossible from the point of view of a point particle, as then the internal current  $J^I$  corresponds to an effective particle momentum,<sup>19-22</sup> and the kink will perform a momentumless motion in the ratchet case. This circumstance raised discussions of whether the observed rectification of the kink motion is due to additional white noise or discretization effects (see, e.g., Ref. 17). However, such a momentumless motion does not contradict the energy balance principles, as there exists an alternative path for the energy flow in the system—the exchange current  $J^E$ , as we demonstrated in the previous section. In the case of biharmonic driving force all the energy is transported through the exchange current, so that the time-averaged current balance equation (16) reads

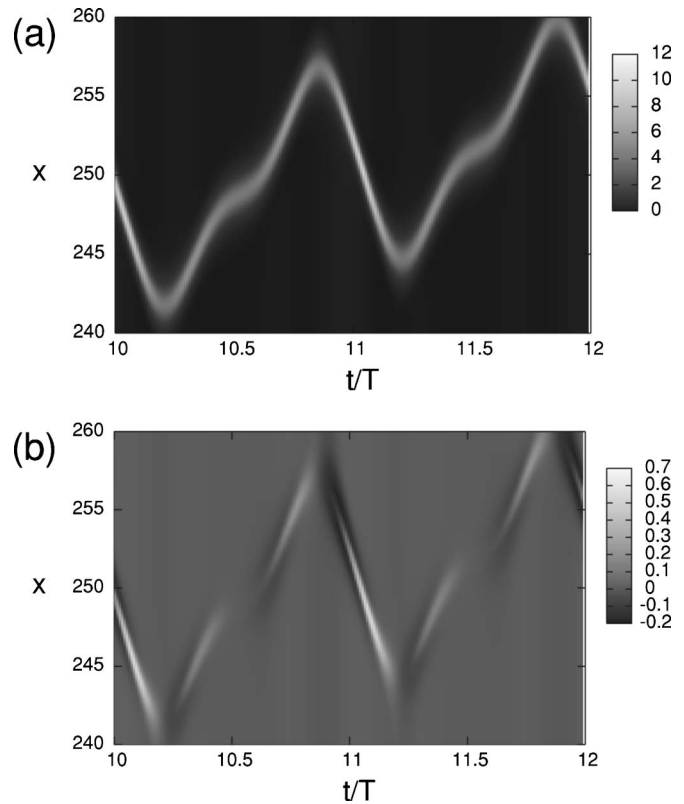


FIG. 3. Space-time evolution of the soliton ratchet with the  $E_1=E_2=0.2$ ,  $\omega=0.1$ ,  $\Theta=0$ ,  $\alpha=0.2$ , and  $L=500$ : (a) Contour plot of the energy density (3) and (b) contour plot of the function  $\phi(x,t)$  defined in Eq. (50).  $x$  values are zoomed near the kink center.

$$\mathcal{J} = \mathcal{J}^E, \quad \mathcal{J}^I = 0. \tag{42}$$

Here we use calligraphic letters to indicate time-averaged quantities,  $\mathcal{J} \equiv (1/T)^2 \cdot \int_0^T dt \int_{t_1}^{t_1+T} dt_1 J(t_1)$  (details of the averaging procedure will be discussed in the following, see also Ref. 16).

Our goal now is to estimate the energy current  $\mathcal{J}$  generated by a moving kink. Taking the system size  $L$  much larger than the characteristic oscillation distance  $L_p$  which the moving kink covers during a single period of the external force, we may assume that far from the kink center the field distribution in space is homogeneous. We separate the field variable  $\varphi(x,t)$  into a localized kink part,  $\varphi^k(x,t)$ , where  $\varphi^k(x \rightarrow 0, t) = 0$ ;  $\varphi^k(x \rightarrow L, t) = Q$ , and a background (vacuum) part  $\varphi^v(t)$  which depends only on time<sup>21</sup>:

$$\varphi(x,t) = \varphi^k(x,t) + \varphi^v(t). \tag{43}$$

The vacuum part must satisfy Eq. (1) in the absence of the kink, i.e., when  $Q=0$ . Therefore it does not contribute to any energy transport.<sup>8</sup>

On the attractor the dynamics of the system (1) is given by

$$\varphi^k(x, t + T) = \varphi^k(x - \mathcal{V}T, t), \quad \varphi^v(t + T) = \varphi^v(t), \tag{44}$$

where  $\mathcal{V}$  is the averaged kink velocity. Here we assume that the ac driving force  $E(t)$  oscillates slowly,  $T \gg 1$ , so that we can continue periodic solution from the adiabatic limit<sup>28</sup> (this is confirmed by our numerical simulations, see Fig. 3). Note

that all integral system characteristics, such as the total energy of the system, the kink velocity, the energy current, etc., are periodic functions of time with the period  $T$ .

As the total system energy  $W$  (11) is not conserved, we cannot introduce instantaneous energy currents. However, as  $W$  is a time-periodic function on the kink attractor solution, we estimate currents by considering energy density distribution changes over the period of attractor, when the total system energy is restored. Assuming that  $x=0$  corresponds to a kink tail point, the amount of energy  $\Delta w(x, t)$ ,

$$\begin{aligned} \Delta w(x, t) &= \int_0^x [\rho(x', t) - \rho(x', t + T)] dx' \\ &= - \int_0^x dx' \int_t^{t+T} \rho_t(x', t') dt' \end{aligned} \tag{45}$$

which the part of the system  $[0, x]$  loses or gains during one period  $T$  has to be transported through the point  $x$  by the energy current  $j(x, t) = \Delta w(x, t)/T$ . Both quantities,  $j(x, t)$  and  $\Delta w(x, t)$ , are obviously periodically dependent on the reference time  $t$ . However, it is misleading to associate them with any instantaneous characteristics of the system, as  $\Delta w(x, t)$  is defined on the timescale of the attractor period  $T$ . In order to eliminate the dependence on reference time  $t$  we average both quantities over the period  $T$ . Finally, the total averaged energy current in the system is obtained by the additional integration over the space

$$\mathcal{J} = \frac{1}{T} \int_0^L dx \int_0^T dt j(x, t), \quad j(x, t) = \frac{1}{T} \Delta w(x, t). \tag{46}$$

Using Eqs. (1) and (44) and the multiplicative integration rule<sup>23</sup> we finally obtain (see the Appendix for details)

$$\mathcal{J} = \mathcal{V} \left\langle \int_0^L \rho[\varphi(x, t)] dx - L\rho[\varphi^v(t)] \right\rangle_T, \tag{47}$$

with  $\langle \dots \rangle_T = 1/T \int_0^T \dots dt$ . As before, the difference between the total system energy  $W$  and the background energy  $W_0$ , averaged in the rhs of Eq. (47), denotes the kink energy  $W^k$ . Therefore, the general result for the total energy current, given in Eq. (14), still holds in this case, if *using averaged values*.<sup>29</sup>

Using the results (45) and (46) we can now derive an expression for the averaged exchange current  $\mathcal{J}^E$  from the energy balance equation (4)

$$\mathcal{J}^E = \frac{1}{T} \int_0^T dt \int_0^L dx j^E(x, t), \tag{48}$$

$$j^E(x, t) = \frac{1}{T} \int_t^{t+T} dt' \int_0^x dx' \phi(x', t'), \tag{49}$$

$$\phi(x, t) = \phi[\varphi] = \alpha \varphi_t^2 - E(t) \varphi_t. \tag{50}$$

Note, that similar to previously defined  $j(x, t)$  in Eq. (47), the quantity  $j^E(x, t)$  cannot be treated as an instantaneous current density value.

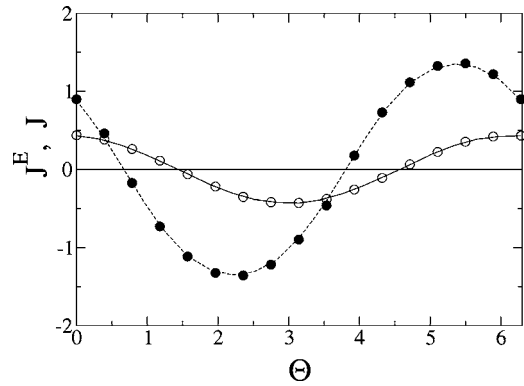


FIG. 4. Numerically computed average values of the exchange current  $\mathcal{J}^E$  (lines) and total current  $\mathcal{J}$  (circles) as a function of the driving force parameter  $\Theta$  for  $\alpha=0.2$  (solid line, filled circles) and  $\alpha=0.05$  (dashed line, open circles). Other parameters are the same as in Fig. 3.

Again, using the multiplicative integration rule,<sup>23</sup> Eqs. (48)–(50) can be reduced to the more compact form (see the Appendix for details)

$$\mathcal{J}^E = - \left\langle \int_0^L [\phi(x - \mathcal{V}T, t) - \phi^v(t)] [x - \mathcal{V}t] dx \right\rangle_T, \tag{51}$$

where  $\phi^v(t) \equiv \phi[\varphi^v(t)]$ .

The appearance of a nonzero exchange current in the system is mediated by a spatially and temporally inhomogeneous energy exchange between the moving kink and the external degrees of freedom. The information about the energy exchange process is contained in the function  $\phi(x, t)$  (50) introduced earlier. In Fig. 3(b) the space-time evolution of  $\phi$  is plotted. The energy is exchanged and transported in a cyclic way: first the kink absorbs energy in its rare tail, then it releases energy in its front, then it absorbs energy in its front and finally releases energy in the rare tail.

The numerical simulations of the kink dynamics (1) confirm that the balance between averaged values of the total and exchange currents holds, see Fig. 4. The absolute values of the exchange current increased, as compared to the case of a constant driving force (cf. with Table I). It may be due to the excitation of kink shape modes, which are clearly observed in Fig. 3—the kink is much more compressed when moving opposite to its average propagation direction as compared to the times when it moves in the same direction.

Note that the rectification effect vanishes at a certain value of the phase mismatch  $\Theta$  between the two components of the driving force. This value depends on the damping constant  $\alpha$ . That is due to another symmetry property of the system (1) in the Hamiltonian limit  $\alpha \rightarrow 0$ . Indeed, in that limit the system possesses the time-reversal symmetry  $t \rightarrow -t$ . That symmetry operation changes the sign of the kink velocity (40), provided the driving force is taken to be symmetric in time,  $E(-t) = E(t)$ . Therefore, in the Hamiltonian limit the rectification effect should disappear at  $\Theta = 0, \pi$ . In the underdamped regime  $\alpha \ll 1$  this effect persists at some value of  $\Theta$  close to  $\Theta = 0, \pi$ .<sup>8</sup>

If a dc component is added to the biharmonic driving force (41), a careful tuning of the parameters can lead to an exact cancellation of both dc and ac force components, so

that  $\mathcal{V}=0$ . Then the averaged total current  $\mathcal{J}$  (47) is exactly zero. However, according to Eq. (19), the internal current is  $\mathcal{J}^I = -QE^{\text{stop}}/\alpha$ , where  $E^{\text{stop}}$  is the dc component of the driving force. This implies an exact balance between the two nonvanishing current components

$$\mathcal{J}=0, \quad \mathcal{J}^E = -\mathcal{J}^I. \quad (52)$$

For example, taking parameter values from Fig. 3, we found  $E^{\text{stop}} \approx 0.01705$  and  $\mathcal{J}^E = -\mathcal{J}^I \approx 0.536$ . Note also, that for any  $0 < E < E^{\text{stop}}$  the sign of the total momentum of the system  $\mathcal{J}$  is *opposite* to the sign of the kink velocity  $\mathcal{V}$ , and the internal current is pumping energy in a direction opposite to the kink motion.

## V. EFFECTS OF SPATIAL DISCRETIZATION

Up to now we discussed the energy flow due to kink motion in a spatially extended *continuous* system. It is known, that the spatial discreteness of a system can drastically change the soliton dynamics.<sup>30</sup> By breaking translational invariance of the system, discreteness induces a Peierls-Nabarro potential which strongly influences the translational motion of the kink.<sup>30</sup> It is also known, that additional internal modes of the kink may appear in discrete systems.<sup>31</sup> Their existence can essentially modify energy exchange mechanisms between the moving kink and external driving forces and damping. As a consequence, the relative contributions of the internal and exchange currents to the total energy current can be strongly changed in the discrete case both for dc and ac driving forces.

Let us consider the discrete version of Eq. (1) also known in literature as the damped and driven Frenkel-Kontorova chain,<sup>32</sup>

$$\ddot{\varphi}_n - C^2(\varphi_{n+1} + \varphi_{n-1} - 2\varphi_n) = -\alpha\dot{\varphi}_n - \sin \varphi_n + E(t). \quad (53)$$

It has been used in solid state theory for modeling dislocation dynamics in crystals. This equation also describes fluxon dynamics in one-dimensional arrays of coupled Josephson junctions.<sup>33</sup> It is important to note, that Eq. (53) is often used for numerical simulations of the original continuous sin-Gordon system (1), where  $C \sim 1/h$  is the inverse mesh size or the lattice spacing (i.e.,  $C \rightarrow \infty$  corresponds to the continuous limit). In this respect it is also important to investigate possible effects of discretization which might appear during the numerical calculation of energy currents of an underlying spatially continuous system.

In order to relate the previous results for the continuous sin-Gordon model (1) to the discrete system (53), we use the transformation  $x \rightarrow n/C$ ,  $\varphi(x, t) \rightarrow \varphi(n/C, t) = \varphi_n(t)$ . Thus, all spatial derivatives should be replaced by finite differences weighted by the factor  $1/h=C$ , whereas all spatial integrals should be replaced by discrete sums over lattice sites with the weight factor  $1/C$ . With that we obtain the following discretized versions for the internal (5) and total (47) energy currents:

$$J^I = \frac{1}{C} \sum_n j_n^I, \quad (54)$$

$$J = V_d \sum_n [\rho_n - N\rho^v], \quad (55)$$

where  $V_d$  is the kink velocity calculated in units of lattice site differences per time. The local internal current  $j_n^I$  and energy density  $\rho_n$  are yet to be defined.

We note, that the Frenkel-Kontorova model (53) corresponds to the Hamiltonian

$$H = \sum_n \rho_n = \sum_n \left\{ \frac{\dot{\varphi}_n^2}{2} + \frac{C^2}{4} [(\varphi_{n+1} - \varphi_n)^2 + (\varphi_n - \varphi_{n-1})^2] + 1 - \cos(\varphi_n) \right\}. \quad (56)$$

Following essentially the same steps as in Sec. II, we can derive the discrete version of the energy balance equation (4) for the discrete energy density  $\rho_n$  (energy of an individual lattice site),

$$\frac{d\rho_n}{dt} = -C(j_n^I - j_{n-1}^I) - \alpha\dot{\varphi}_n^2 + E(t)\dot{\varphi}_n, \quad (57)$$

$$j_n^I = \frac{C}{2}(\dot{\varphi}_{n+1} + \dot{\varphi}_n)(\varphi_{n+1} - \varphi_n). \quad (58)$$

The internal current density  $j_n^I$  (also known as the local heat flux<sup>34</sup>) is the discrete analogue of the internal current density (5) of the continuum case.

In contrast to the continuum limit, it is not straightforward to define a discrete version of the exchange current on the basis of the last two terms in the rhs of the balance equation (57). However, the exchange current can be computed via the difference between the total and internal currents,  $J^E = J - J^I$ .

In Fig. 5 the dependencies of the computed energy currents on the discretization parameter  $C$  are plotted for the cases of dc and ac external driving forces. Increasing  $C$ , in both cases all the currents clearly converge to the corresponding values obtained in the continuum limit: in the dc case the dominant energy pathway is realized through the internal current, whereas in the ac case the only remaining path for energy transport is mediated by the exchange current. In the latter case the internal current scales down to zero as  $J^I \sim C^{-2}$  for  $C^2 \geq 10$ , which follows from the approximation of integrals by discrete sums.<sup>23</sup> Spatial discretization can drastically change the ratio between the two currents when  $C^2 \leq 10$  both in the case of a constant external bias, and in the case of a soliton ratchet.<sup>8</sup> As for these values of  $C$  the Peierls-Nabarro potential is still exponentially small,<sup>36</sup> the cause of the corrections is simply the change of the kink shape which is of order  $1/C^2$ .<sup>37</sup>

## VI. CONCLUSIONS

We discussed the issue of soliton-assisted energy transport in spatially extended systems with external driving and damping. Considering the topological soliton (kink) motion in the well-known sin-Gordon model, we showed, that the conventional description of energy transport based on the total field momentum does not provide one with the correct



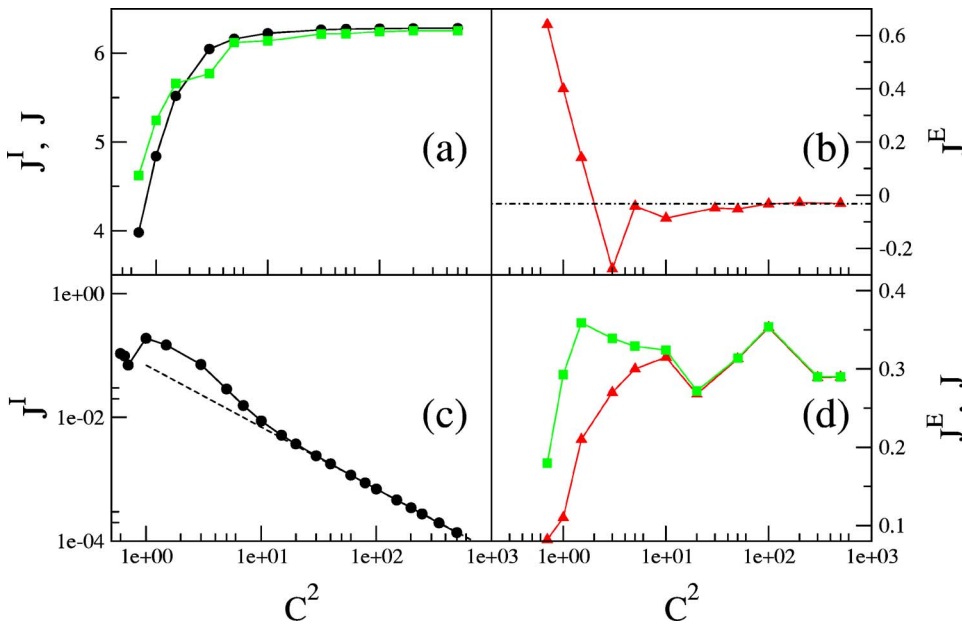


FIG. 5. The internal (filled circles), the exchange (triangles) and the total (squares) energy currents as functions of the discretization parameter  $C^2$ . (a) and (b): the case of the dc external force  $E=0.2$ ; (c) and (d): the case of the biharmonic driving force (41) with  $E_1=E_2=0.2$  and  $\Theta=0$ .  $\alpha=0.2$  for all cases. The dash-dotted line in (b) indicates the exchange current value,  $J^E \approx -0.032\ 012\ 8$ , calculated for the continuum limit within the pendulum approach (see Table I). The dashed line in (c) corresponds to the power-law asymptotic  $J \sim C^{-2}$ .

value of energy flux in the system. In particular, in the case of a directed soliton motion under the influence of time-periodic external forces with zero mean, the averaged value of the total field momentum is known to be strictly zero,<sup>16,17,20,21</sup> whereas the energy transport associated with the soliton motion is obviously nonzero. We identified a new energy pathway—the *exchange current*—which is entirely mediated by the spatial and temporal inhomogeneity of the system state. Even for the case of a dc external force, the exchange current is found to be small but nonzero. Combining both dc and ac driving we obtain situations when the total field momentum is nonzero but the kink does not move on average or moves even in the direction opposite to the field momentum.

The approach to the energy transport in spatially extended systems which is based solely on the consideration of the total field momentum reduces the kink motion to that of a point particle. However, the soliton motion in presence of ac driving forces is always accompanied by the excitation of internal modes,<sup>35</sup> which makes the dynamical properties of the moving soliton essentially different from those of a point particle. Although we stress here that, even in cases where no shape modes are excited, the total field momentum is not sufficient to obtain the total energy current (see Sec. III). It is the spatial extent of the soliton which makes the difference for a damped and driven moving soliton. The appearance of a nonzero exchange current in the case of the constant driving force is connected to the asymmetry of a moving kink profile. We believe, that, in the limit of small dissipation and damping, the exchange current could be estimated perturbatively, provided the ansatz for the moving kink solution is modified in order to account for an asymmetric correction. The corresponding perturbative analysis is a matter of another important investigation, which lies, however, beyond the scope of the present work.

The relative contributions of the two current components, the internal and the exchange one, can change when considering spatially discrete systems (see Sec. V). In par-

ticular, for the soliton ratchet case, discreteness induced corrections to the internal current invalidate Eq. (6), so that  $J^I$  also contributes to the total energy flow. This explains earlier obtained numerical results from Ref. 8.

The physical origin of the exchange current is tightly connected with the physics of the external drive and the way it couples to the system under consideration. It corresponds to an energy flow between the driver and the system, which is inhomogeneous in time and space. In other words, the energy flows at some time and in some position from the system into the driver, and is returned into the system at another time and another position. The sum of the internal and the exchange currents gives then the total current.

Finally, we would like to note that our results are also instructive for the general case of spatially extended systems coupled to external driving forces or other degrees of freedom (see, e.g., Refs. 18 and 38). We also mention that the damped and driven sin-Gordon system in Eq. (1), as well as its discretized version in Eq. (53), are relevant physical models of annular<sup>12,13</sup> and coupled<sup>33</sup> Josephson junction oscillators, respectively. Therefore, an intriguing question rises about the possibility of detection of the new exchange current mechanism on the basis of available experimental data (current-voltage characteristics, spectra of emitted radiation, etc.). Indeed, as directed soliton motion is observed in such experiments, the internal and exchange currents have a clear physical meaning, though probably not easy to measure.

**APPENDIX: DERIVATION OF TOTAL AND EXCHANGE CURRENTS FOR TIME-PERIODIC DRIVING**

Using Eq. (45), let us rewrite the expression (47) for the energy current  $\mathcal{J}$  in the following form:

$$\mathcal{J} = \frac{1}{T^2} \int_0^T dt \int_0^L dx \int_0^x dx' [\rho(x', t) - \rho(x', t + T)]. \quad (A1)$$

According to the multiplicative integration rule<sup>23</sup>

$$\begin{aligned} & \int_0^L dx \int_0^x dx' [\rho(x', t) - \rho(x', t+T)] \\ &= \int_0^L (L-x) [\rho(x, t) - \rho(x, t+T)] dx. \end{aligned} \quad (\text{A2})$$

As the total energy of the system  $W$  is a periodic function with period  $T$ , the integral  $\int_0^L L[\rho(x, t) - \rho(x, t+T)] dx = L[W(t) - W(t+T)] \equiv 0$ . Thus, expression (A1) is reduced to

$$\mathcal{J} = \frac{1}{T^2} \int_0^T dt \int_0^L x [\rho(x, t) - \rho(x, t+T)] dx. \quad (\text{A3})$$

Let us introduce the energy-weighted center of kink

$$\hat{X}(t) = \frac{\int_0^L x [\rho(x, t) - \rho^v(t)] dx}{\int_0^L [\rho(x, t) - \rho^v(t)] dx}, \quad (\text{A4})$$

where  $\rho^v(t) \equiv \rho[\varphi^v(t)]$ . Then we obtain

$$\mathcal{J} = \frac{1}{T^2} \int_0^T dt \int_0^L [\rho(x, t) - \rho^v(t)] \cdot [\hat{X}(t+T) - \hat{X}(t)] dx. \quad (\text{A5})$$

As  $[\hat{X}(t+T) - \hat{X}(t)] = \mathcal{V}T$ , finally we arrive to the following expression for the total energy current:

$$\mathcal{J} = \frac{\mathcal{V}}{T} \int_0^T dt \int_0^L [\rho(x, t) - \rho^v(t)] dx. \quad (\text{A6})$$

In a similar way one can derive the compact expression (51) for the exchange current. We rewrite the expression (48) in the following form:

$$\begin{aligned} \mathcal{J}^E &= \frac{1}{T^2} \int_0^L dx \int_0^x dx' \left\{ \int_T^{2T} dt \int_T^t \phi(x', t') dt' \right. \\ &\quad \left. - \int_0^T dt \int_0^t \phi(x', t') dt' + T \int_0^T \phi(x', t) dt \right\}. \end{aligned} \quad (\text{A7})$$

Applying twice the multiplicative integration rule, we obtain

$$\begin{aligned} \mathcal{J}^E &= \frac{1}{T^2} \int_0^L dx (L-x) \int_0^T dt \{ T\phi(x, t+T) \\ &\quad - t[\phi(x, t+T) - \phi(x, t)] \}. \end{aligned} \quad (\text{A8})$$

By introducing the center of kink  $\tilde{X}(t)$  weighted by function  $\phi(x, t)$  in analogy to (A4), and using  $[\tilde{X}(t+T) - \tilde{X}(t)] = \mathcal{V}T$ , expression (A8) becomes

$$\begin{aligned} \mathcal{J}^E &= -\frac{1}{T} \int_0^T dt \int_0^L \phi(x - \mathcal{V}T, t) \cdot (x - \mathcal{V}t) dx \\ &\quad - \frac{\mathcal{V}}{T} \int_0^T t dt \int_0^L \phi[\varphi^v(t)] dx. \end{aligned} \quad (\text{A9})$$

Taking into account that  $\langle \phi[\varphi^v(t)] \rangle_T \equiv 0$ , we finally obtain expression (51) for the exchange current.

<sup>1</sup>See, e.g., M. Remoissenet, *Waves Called Solitons: Concepts and Experiments* (Springer, Berlin, 1996).

<sup>2</sup>N. J. Zabusky and M. D. Kruskal, Phys. Rev. Lett. **15**, 240 (1965).

<sup>3</sup>D. K. Campbell, J. F. Schonfeld, C. A. Wingate, Physica D **9**, 1 (1983); M. Peyrard and D. K. Campbell, *ibid.* **9**, 33 (1983); D. K. Campbell, M. Peyrard, and P. Sodano, *ibid.* **19**, 165 (1986).

<sup>4</sup>Y. S. Kivshar, D. E. Pelinovsky, T. Cretegny, and M. Peyrard, Phys. Rev. Lett. **80**, 5032 (1998).

<sup>5</sup>F. Marchesoni, Phys. Rev. Lett. **77**, 2364 (1996).

<sup>6</sup>M. Salerno and N. R. Quintero, Phys. Rev. E **65**, 025602 (2002).

<sup>7</sup>G. Costantini, F. Marchesoni, and M. Borromeo, Phys. Rev. E **65**, 051103 (2002).

<sup>8</sup>S. Flach, Y. Zolotaryuk, A. E. Miroshnichenko, and M. F. Fistul, Phys. Rev. Lett. **88**, 184101 (2002).

<sup>9</sup>M. Salerno and Y. Zolotaryuk, Phys. Rev. E **65**, 056603 (2003).

<sup>10</sup>C. R. Willis and M. Farzaneh, Phys. Rev. E **69**, 056612 (2004).

<sup>11</sup>L. Morales-Molina, N. R. Quintero, F. G. Mertens, and A. Sánchez, Phys. Rev. Lett. **91**, 234102 (2003).

<sup>12</sup>A. V. Ustinov, C. Coqui, A. Kemp, Y. Zolotaryuk, and M. Salerno, Phys. Rev. Lett. **93**, 087001 (2004).

<sup>13</sup>M. Beck, E. Goldobin, M. Siegel, R. Kleiner, and D. Koelle, Phys. Rev. Lett. **95**, 090603 (2005).

<sup>14</sup>P. Hänggi and R. Bartussek, in *Nonlinear Physics of Complex Systems*, edited by J. Parisi, S. C. Müller, and W. Zimmermann, Lecture Notes in Physics (Springer, Berlin, 1996), Vol. 476, p. 294 P. Reimann, Phys. Rep. **361**, 27 (2002); P. Hänggi, F. Marchesoni, and F. Nori, Ann. Phys. **14**, 51 (2005).

<sup>15</sup>S. Flach, O. Yevtushenko, and Y. Zolotaryuk, Phys. Rev. Lett. **84**, 2358 (2000); S. Denisov, S. Flach, A. A. Ovchinnikov, O. Yevtushenko, and Y. Zolotaryuk, Phys. Rev. E **66**, 041104 (2002).

<sup>16</sup>S. Denisov, S. Flach, and A. Gorbach, Europhys. Lett. **72**, 183 (2005).

<sup>17</sup>N. R. Quintero, B. Sanchez-Rey, and J. Casado-Pascual, Phys. Rev. E **71**, 058601 (2005); C. R. Willis and M. Farzaneh, *ibid.* **71**, 058602 (2005).

<sup>18</sup>I. V. Barashenkov and E. V. Zemlyanaya, SIAM J. Appl. Math. **64**, 800 (2004).

<sup>19</sup>R. K. Dodd, *Solitons and Nonlinear Wave Equations* (Academic, London, 1982).

<sup>20</sup>E. Joergensen, V. P. Koshelets, R. Monaco, J. Mygind, and M. R. Samuelsen, Phys. Rev. Lett. **49**, 1093 (1982).

<sup>21</sup>O. H. Olsen and M. R. Samuelsen, Phys. Rev. B **28**, 210 (1983).

<sup>22</sup>L. L. Bonilla and B. A. Malomed, Phys. Rev. B **43**, 11539 (1991); D. Cai, A. Sánchez, A. R. Bishop, F. Falo, and L. M. Floría, *ibid.* **50**, 9652 (1994).

<sup>23</sup>I. S. Gradshteyn and I. M. Ryzhik, *Table of Integrals, Series, and Products* (Academic, New York, 1994).

<sup>24</sup>C. M. Falco, Am. J. Phys. **44**, 733 (1976).

<sup>25</sup>M. Levi, F. C. Hoppensteadt, and W. L. Miranker, Q. Appl. Math. **36**, 167 (1978).

<sup>26</sup>E. Ben-Jacob, D. J. Bergman, B. J. Matkowsky, and Z. Schuss, Phys. Rev. A **26**, 2805 (1982).

<sup>27</sup>All numerical simulations were made with use of the discretized version of Eq. (1). The details of discretization are discussed in Sec. V.

<sup>28</sup>E. Goldobin, B. A. Malomed, and A. V. Ustinov, Phys. Rev. E **65**, 056613 (2002).

<sup>29</sup>In the nonadiabatic regime, when the condition of the periodicity (44) is not guaranteed any more, our approach is still applicable with the replacing of the time averaging over the period  $T$  by the asymptotic averaging,  $\langle \dots \rangle = \lim_{T \rightarrow \infty} 1/T \int_0^T \dots dt$ .

<sup>30</sup>O. M. Braun and Yu. S. Kivshar, Phys. Rep. **306**, 1 (1998).

<sup>31</sup>O. M. Braun, Yu. S. Kivshar, and M. Peyrard, Phys. Rev. E **56**, 6050 (1997).

<sup>32</sup>Ya. I. Frenkel and T. Kontorova, Zh. Eksp. Teor. Fiz. **8**, 1340 (1938).

<sup>33</sup>A. V. Ustinov, M. Cirillo, B. H. Larsen, V. A. Oboznov, P. Carelli, and G. Rotoli, Phys. Rev. B **51**, 3081 (1995).

<sup>34</sup>S. Lepri, R. Livi, and A. Politi, Phys. Rep. **377**, 1 (2003).

<sup>35</sup>L. Morales-Molina, N. Quintero, A. Sanchez, and F. G. Mertens, Chaos **16**, 013117 (2006).

<sup>36</sup>S. Flach and C. R. Willis, Phys. Rev. E **47**, 4447 (1993).

<sup>37</sup>S. Flach and K. Kladko, Phys. Rev. E **54**, 2912 (1996).

<sup>38</sup>A. L. Sukstanskii and K. I. Primak, Phys. Rev. Lett. **75**, 3029 (1995).